NUMERICAL INVESTIGATION ON THE STRESS DISTRIBUTION IN HOLLOW COMPOSITE PROFILES DUE TO OVERMOLDING

Alexander Liebsch[1], Robert Kupfer[1], Andreas Hornig[1], Maik Gude[1]

[1]Technische Universität Dresden, Institute of Lightweight Engineering and Polymer Technology
Holbeinstraße 3, 01307 Dresden, Germany
Email: alexander.liebsch@tu-dresden.de, web page: http://tu-dresden.de/mw/ilk

Keywords: finite elements, process simulation, injection molding, thermoplastic structures, DEM

ABSTRACT

Complex-shaped hollow profiles of continuous fiber-reinforced thermoplastics are predestined for high-volume manufacturing of lightweight structures with exceeding stiffness and strength. To apply additional functional elements like ribs, such profiles can be overmolded from the outside with thermoplastic material by injection molding. To prevent the hollow profiles from collapsing under the high local injection pressures, they have to be supported by a core from the inside. For complex-shaped hollow profiles, free flowing core materials like particle or fluid media appear particularly suitable, as they enable a filling of the hollow profiles with undercuts or changes in the cross section. In the present work, a method to analyze the deformation behavior of a hollow profile and the supporting core during the injection molding process was approved. Therefore, the filling-time and pressure dependent loading on the hollow profile was gained from form-filling analyses. Afterwards, these loads were transferred into structural analyses to determine the load distribution in the hollow profile and the resulting loads on the core. For the simulation of the particle core a discrete element method (DEM-) model was applied. The fluid core was simulated by means of smoothed particle hydrodynamics (SPH). The results, which show a significant different deformation behavior of both core systems, are discussed.

1 INTRODUCTION

At present, continuous fiber-reinforced composite structures are mostly made using thermoset matrix materials. As curing processes are often time-consuming, thermoset matrices are only partially appropriate for high volume production [1]. The substitution of thermosets by thermoplastic matrices overcomes this disadvantage by offering new processing technologies with cycle times less than 60 seconds [2]. One of the most common manufacturing processes is stamp-forming of thermoplastic composite (TPC-) sheets. These fully impregnated textiles are warmed up above the melting temperature of the thermoplastic matrix. Afterwards, the softened PTC-sheets are transferred into a pressing tool. By closing the tool subsequently the TPC-sheets are shaped three-dimensionally and cool down inside the pressing tool.

The combination of the stamp-forming process with injection molding was the subject of numerous developments within the last years [3]. Thereby, the textiles are shaped inside an injection molding tool and are overmolded inside the same tool afterwards. Due to the contact of the heated TPC-sheets and the injection molding material, an adhesive joint is established between both components. This technology allows the production of complex shaped structures with a high load carrying capacity within a short cycle time.

Recent investigations show, that the overmolding process cannot be simply applied to thermoplastic composite hollow profiles [4]. The injection pressure leads to high surface loadings on the hollow profile and causes large deformations of the hollow profile or even its collapsing. To support the hollow profile, adapted core systems have to be developed. Besides the supporting of the hollow profile, an easy insertion of the core into the hollow profile has to be guaranteed. Due to the geometric complexity of the most technical profiles, free flowing core media are particularly suitable. In [4], cores based on incompressible fluids and particles were investigated experimentally. In these

investigations it was shown, that particle cores support the hollow profile well and the collapsing could be prevented. With the usage of an incompressible fluid, the collapsing of the hollow profile could be prevented as well. However, it was observed that the injection molded substructure was not completely filled. Furthermore, fiber breakages occurred at areas close to the unfilled substructures. It was assumed, that the local external injection pressure is converted into a global internal fluid pressure which presses the hollow profile against the tool's surface. Furthermore, it was suspected that the hollow profile is pressed into the unfilled areas of the cavity by the internal fluid pressure which leads to fiber breakages and insufficient overmolding (Figure 5).

A method for further investigations of the behavior of a hollow profile with two different core types during the injection molding process was approved within the present work. Therefore, filling simulations were carried out to estimate the loads on the hollow profile during overmolding. Afterwards, the loads were transferred to structural simulations to investigate the behavior of the hollow profile and the internal core during injection molding. For the simulation of the particle system, the discrete element method (DEM) was used. The simulation of the liquid was performed using smoothed particle hydrodynamics (SPH) with an incompressible material definition. The results are discussed and compared with the observed failure phenomena in [4].

2 NUMERICAL INVESTIGATIONS

The investigations of the present work were carried out using a two-step-approach. At first, filling simulations were conducted. These simulations provide the loads, acting on the hollow profile during injection molding. The loads were extracted and transferred to structural simulations to investigate the resulting deformation of the hollow profile in dependency on the core behavior.

2.1 FILLING SIMULATIONS

The investigations are performed for a generic hollow profile (Figure 1) that consists of a hollow profile with varying cross sections (circular to hexagonal to circular shape). The profile is made of polyamide 6 (PA6) glass-fiber hybrid yarns with a fiber volume content of 50 % and is consolidated in a variotherm bladder inflation process. The injection molded structure consists of small- and large-area substructures and is filled by a pin gate. As the injection molding material, a PA66/PA6 (GRILON TSS/4, EMS-CHEMIE) was used.

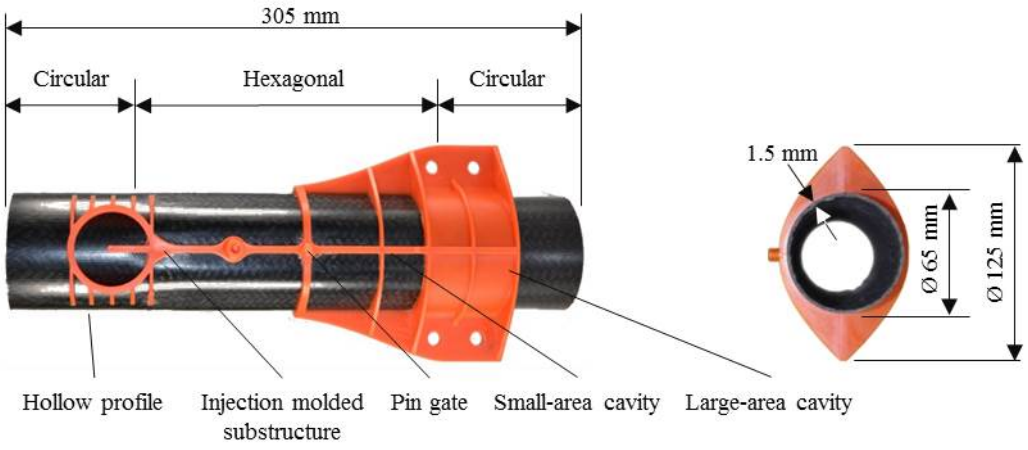

Figure 1: Generic hollow profile made of PA6-glass-fiber hybrid yarn with overmolded substructures.

The filling simulations were conducted using the software Autodesk SIMULATION MOLDFLOW SYNERGY 2014 [11]. The properties of the chosen polymer were taken from the provided database of MOLDFLOW. To obtain the time dependent pressure on the hollow profile, a coreshift analysis was performed. Using this analysis, the appearing loads on an injection molding insert during the process

can be examined and the displacement of the insert caused by unequal force transmission of the flowing plastic material can be estimated. To determine the transient pressure profile acting on a hollow profile that is supported ideally, the hollow profile was modeled as a rigid part with a temperature of 25 °C. The loads were exported every 2 % of the filling time. Numerical parameter studies were performed to identify suitable process parameters for filling the filigree structure. The obtained process parameters are summarized in Table 1.

Variable	Unit	Value
Mold surface temperature	[°C]	120
Melt temperature	[°C]	285
Maximum machine injection stroke	[mm]	150
Maximum machine injection rate	[cm³ / s]	106
Machine screw diameter	[mm]	30
Maximum machine injection pressure	[MPa]	235
Maximum machine clamp force	[ton]	30

Table 1: Determined process data for the injection molding process.

Figure 2 shows the time dependent pressure distribution acting on the hollow profile at three different points (1: gate, 2: large-area cavity, 3: far from the gate). It can be observed that the load acting on the hollow profile increases rapidly in the area of the gate during the first 0.5 seconds of the filling phase. Afterwards, the intensity of the load increase declines. During the packing phase, the applied pressure on the profile increases rapidly to its maximum of 13 MPa. The load distributions at point 2 and 3 have qualitatively the same gradient as at point 1 but differ quantitatively. As expected, the load values are less at point 2 and 3 compared with point 1, where the pressure maximum is located. To identify the influence of the load application on the supporting core and to demonstrate the general simulation approach, the transient load profile of point 1 was exemplarily analyzed for the first 0.39 seconds which represents the first 10 % of the filling process (highlighted in Figure 2, right).

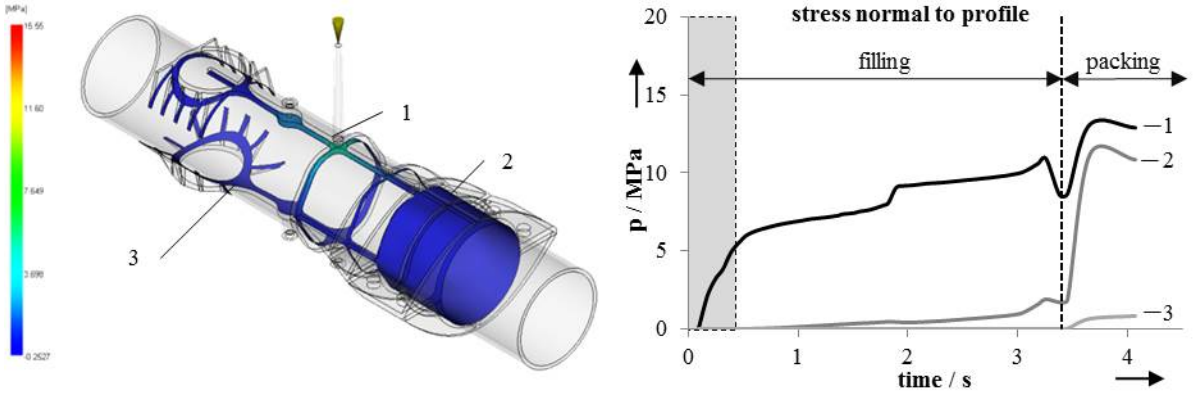

Figure 2: Pressure distribution on the hollow profile after 0.39 s (left); time dependent pressure acting on hollow profile (right).

2.2 NUMERICAL SIMULATIONS OF STRUCTURAL BEHAVIOR

The finite element software ABAQUS / EXPLICIT 6.13 [8] was used to investigate the structural behavior of the hollow profile during the injection molding process. Two models were generated to examine the response of both, the particle and the liquid core. For both a basic structural model (Figure 3) representing the hollow profile and the tool's surface was used, consisting of shell elements (S4R) with lamina material properties (Table 2) for the hollow profile. The assigned shell thickness is 1.5 mm with a material orientation of ± 45° referred to the longitudinal axis of the profile. The contact surface of the injection molding tool is represented by discrete rigid elements (R3D4). The model

contains two cover faces modelled with discrete rigid elements (R3D4) at the ends of the hollow profile to encapsulate the enclosed core material.

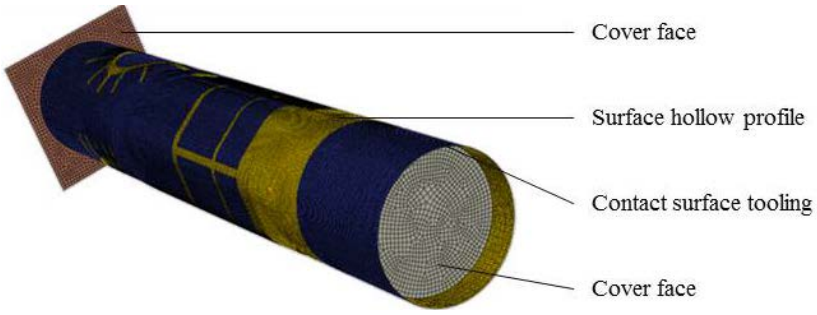

Figure 3: Basic model of the hollow profile for the numerical simulation.

Variable	Unit	Value
E_1	[GPa]	32.8
E_2	[GPa]	9.9
G_{12}	[GPa]	3.8
G_{13}	[GPa]	3.8
G_{23}	[GPa]	1.2
v	[-]	0.2
ρ	[kg/m³]	1.9e3

Table 2: Material data of the hollow profile.

Investigation of the particle core

The DEM developed by Cundall and Starck [5] is an established numerical method to observe the phenomena occurring in particle systems e.g. the motion of single particles or the load distribution within a granular system. For this meshless simulation method, every particle is modelled separately as a single rigid body which has three translational and three rotational degrees of freedom. The motion of the particles is based on the Newton's law of motion. Due to the rigid characteristic of the particles, the interaction between the particles has to be described in separate contact formulations. A summary of the most common contact laws can be found in [6]. The particles can be shaped in every desired way; the least numerical effort is required using spherical particles [6, 7]. Besides the interaction of the particles itself, the elements can also interact with surrounding structures and can undergo external forces e.g. gravity.

The particle core is modeled using monosized spherical particles with diameters of D_P = 3 mm. In [12], it is shown that spherical particles are suitable to predict the response of granular media. The normal contact forces F_N are calculated using the Hertz contact formulation [13]

$$F_N = \frac{3}{4} E^* \sqrt{R} \sqrt{\delta^3} \tag{1}$$

with the penetration depth of the particles δ, the averaged radius of the particles R and the averaged Young's modulus of the particles E^*. E^* is calculated by

$$\frac{1}{E^*} = \frac{1-\nu_1^2}{E_1} + \frac{1-\nu_2^2}{E_2}, \tag{2}$$

where $\nu_{1,\,2}$ are the Poisson's ratios of the particles in contact (1, 2) and $E_{1,\,2}$ the respective Young's moduli. The tangential contact forces F_T are calculated by ABAQUS embedded tangential contact formulation

$$F_T = \mu F_N, \tag{3}$$

with the friction coefficient μ. The damping of the material is respected by the damping force

$$F_D = D\sqrt{4mk}v_{rel}. \quad (4)$$

Here, D is the damping coefficient, m the particle mass, k the contact stiffness and v_{rel} the relative velocity of the contact partners. To ensure the stability of the DEM simulation, it is necessary to estimate the critical time step. According to [14], the time step for spherical particle can be calculated as

$$t_{crit} \leq 0.17\sqrt{\frac{m}{k}}. \quad (5)$$

As a typical granular material, sand was chosen within the present investigations. The material parameters for sand are taken from [8] and [12]. In Table 3 the material parameter for the particle core are summarized.

Variable	Unit	Value
E	[GPa]	0.30
ρ	[kg/m³]	2.6e3
ν	[-]	0.3
μ	[-]	0.2
r	[mm]	1.5
D	[-]	0.3
Number of particle	[-]	48333
D_P	[mm]	3
t_{crit}	[s]	4.0e-6

Table 3: Material data of the granulate and critical time step.

Since an analytical description of the sphere packing for 3D geometries with varying cross section profiles is challenging, the particles were initially distributed into the hollow profile by dropping within an initial load step [8, 12]. To achieve a realistic compacting of the particles as it would be done in reality by vibration, the friction between the particles was set to zero while filling in. Thereby, the interaction of the particles is dominated by pile effects. A blockade of the particle flow due to frictional effects can be precluded with the result of a denser package of the particles. Prior to the second load step, the cover face was placed on top of the particles and the friction was switched on. Afterwards, the load profile at the injection location was applied.

Figure 4 shows the particle motion due to the load application (top, middle) and the contact pressure of the particles (bottom). The maximum movement of the particles is located nearby the gate and decreases as the distance from the injection location increases. The injection pressure acts locally on the surface of the hollow profile and causes the hollow profile to deform at the area of the gate. As a result, the hollow profile is pressed on the particle core and the load is introduced into the core at this point. It can be seen, that there are no distinct regions of high contact pressures. Thus, a transmission of the external load into the whole core can be deduced. As Figure 4 (middle) illustrates, the particles perform not only translational but also a rotational movements. This rotation is induced by friction forces between the particles. The cover faces encapsulate the particles within the hollow profile and prevent their escape. This encapsulation in combination with the friction between the particles leads to a stabilization of the core. Thus, the core behaves similar to a solid medium. A collapsing of the hollow profile can be prevented as reported in [4].

The deformation of the hollow profile along the top and the bottom side is measured alongside evaluation paths (Figure 4). The deformations are shown in Figure 6 (a, b). It can be seen, that the hollow profile gets deformed primarily inwards at the injection location. The deformations of the other surface areas are negligible.

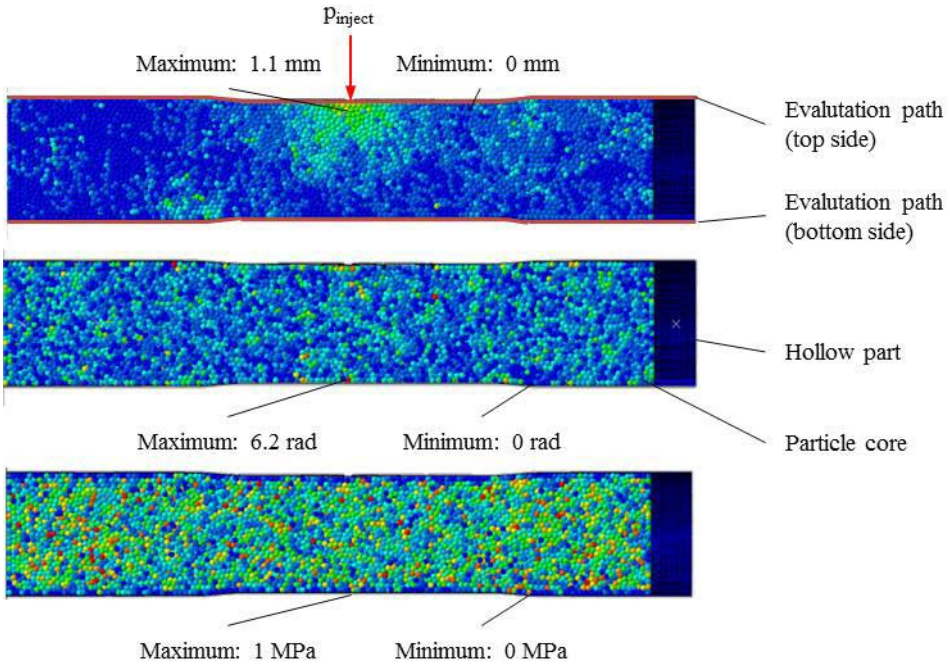

Figure 4: Particle displacements due to injection pressure (top); particle rotation (middle); particle contact pressure (bottom).

Investigation of the fluid core

The simulation of fluids can be executed using SPH which was primarily developed to investigate astronomic effects [7 – 9]. For these meshless simulation methods, the continuum is separated into a discrete number of parcels to overcome numerical problems with large mesh deformations due to flow effects. The SPH is based on the Lagrangian representation of fluid flow where the trajectories of the fluid parcels are observed [10]. In contrast to the DEM, the interaction of the components is not predicated on the colliding of discrete particles. Every parcel of the continuum is assigned a kernel function. With this kernel function, the influence of the parcels on other parcels is described in dependency on the distance to each other. The actual condition of a certain parcel can be determined by summing up the contribution of all adjacent parcels whose kernel functions are unequal zero.

The hydrodynamic behavior of fluids can be described using equations of state (EOS) whereat constitutive equations are used to define the pressure as a value which depends on the density and the internal energy [8, 15]. Adiabatic conditions are assumed. The Mie-Grüneisen-EOS implies a linear energy inclusion and defines the pressure within a compressed medium as

$$P - P_H = \Gamma_0 (E_m - E_H). \tag{3}$$

P_H and E_H represent the Hugoniot pressure and the specific energy, E_m is the energy within the medium. The relation between P_H and E_H can be expressed as followed

$$E_H = \frac{P_H \eta}{2\rho_0}, \tag{4}$$

$$\eta = \frac{1-\rho_0}{\rho},$$

where η is the nominal volumetric compressive strain and ρ_0 the reference density. Γ_0 is the Grüneisen ratio which is expressed as

$$\Gamma = \Gamma_0 \frac{\rho_0}{\rho}. \tag{5}$$

P_H is be defined by

$$P_H = \frac{\rho_0 c_0^2 \eta}{(1-s\eta)^2}. \tag{6}$$

Thus, the pressure in the medium results in

$$P = \frac{\rho_0 c_0^2 \eta}{(1-s\eta)^2}\left(1 - \frac{\Gamma_0 \eta}{2}\right) + \Gamma_0 \rho_0 E_m. \tag{7}$$

For the current investigation it was assumed that the liquid core consists of water. With the assumption that s and Γ_0 equal 0, a simple hydrodynamic behavior of the fluid can be simulated [8]. The viscosity η was set to 1e-8 $N\frac{s}{mm^2}$. In Table 4 the material data chosen for the current investigations are listed.

Variable	Unit	Value
ρ_0	[kg/m³]	996
η	[N s/mm²]	1e-8
s	-	0
Γ_0	-	0
c_0	[mm/s²]	1.45e6

Table 4: Material data of water, [8].

This material model was implemented into a SPH model. It can be seen, that the fluid core behaves differently compared to the particle system (Figure 6 c, d). Similar to the particle core, the hollow profile is deformed inwards at the injection location. However, due to the incompressibility of the fluid, the local external injection pressure is converted into a global internal pressure in the fluid core (Figure 5). This pressure forces the profile to widen. The graphs for the fluid core in Figure 6 c, d show, that the profile is pressed inside non-filled areas of the cavity. As a result of this effect the flow channels can be clogged by the hollow profile and the hollow profile would be overmolded insufficiently. Furthermore, fiber breakages can be induced at the edges of the cavity. These phenomena were also observed in [4].

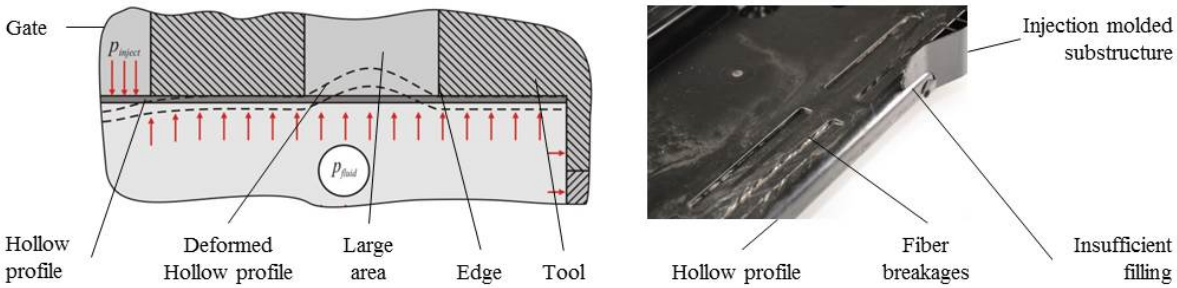

Figure 5: Schematic pressure distribution in the fluid core (left); insufficiently filled injection molded substructure and fiber breakages (right), [4].

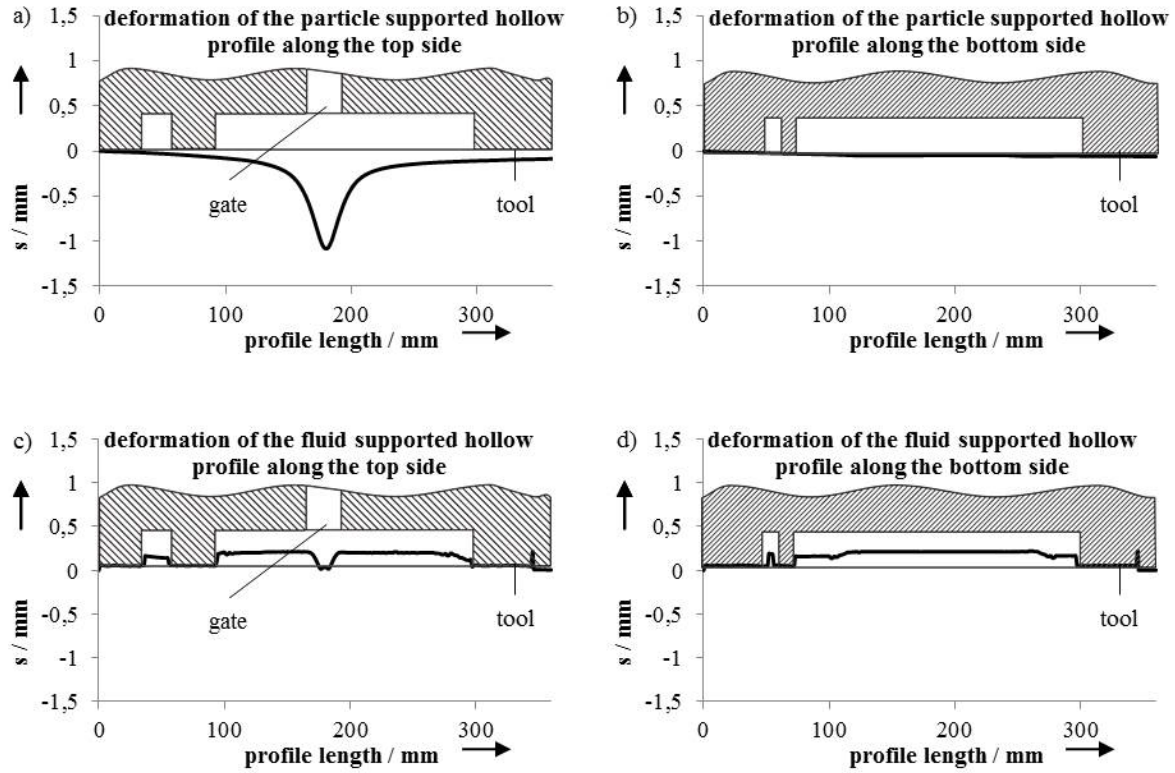

Figure 6: Deformation of the hollow profile due to injection molding; a) evaluation path on the top side for the particle core; b) evaluation path on the bottom side for the particle core; c) evaluation path on the top side for the fluid core; d) evaluation path on the bottom side for the fluid core.

3 CONCLUSIONS

The process of overmolding of TPC-sheets cannot simply be adapted to hollow profiles. Due to the high injection pressure, the hollow profile collapses as reported in [4]. Therefore, it is necessary to use a core that prevents the failure of the hollow profile while overmolding. To support hollow profiles with high complex shapes, free flowing cores like particles or fluids appear useful. It was observed that the supporting behavior of particle and fluid cores differs from each other [4]. Thus, a method to investigate the effects that occur in these types of cores was approved and presented in the current work.

First a form filling simulation was performed to determine the process parameters of the injection molding process and to identify the loads acting on the hollow profile. The loads were transferred to numerical simulations to investigate the deformation behavior of the hollow profile during the injection molding process. The particle core was investigated using DEM and the liquid core with a SPH approach. The results show, that the deformations of the hollow profile supported by particles differ from the deformations behavior of the liquid core.

The particle supported hollow profile deforms inwards at the gate, whereas the remaining surface is almost not deformed. The results show the redistribution of the external applied loads in the core material. Due to the interaction of the particles in combination with the friction between the particles, the core behaves similar to a solid structure. Thereby, the deformation of the hollow profile is limited and a collapsing of the hollow profile during the overmolding process can be prevented.

The simulations of the fluid core show, that the local external injection pressure is converted into a global internal fluid pressure. Thereby the hollow profile is widened by the core system. At areas where the hollow profile is not in contact with the tool’s surface it is pressed inside the flow channels which can result in plugging of the cavity and an insufficient overmolding of the profile. Furthermore, fiber breakages at the edges of the cavity can occur as reported in [4].

Within the presented work, phenomena taking place inside the cores were shown. Further investigations based on these models and concerning the material properties will be conducted to analyze the required property profile of a core for overmolding hollow profiles.

ACKNOWLEDGEMENTS

The authors gratefully acknowledge the financial support of this research by the Deutsche Forschungsgemeinschaft (DFG) within the Collaborative Research Centre (SFB) 639 "Textile-reinforced composites for function-integrating hybrid construction projects in complex lightweight applications", subproject B3, D1, B4.

REFERENCES

[1] VDI e.V., *Werkstoffinnovationen für nachhaltige Mobilität und Energieversorgung*, Düsseldorf, 2014.

[2] R. Kaufmann, T. Bider, E. Bürkle, Leichtbauteile mit Thermoplastmatrix, *Kunststoffe,* **Vol. 101**, **No. 3**, 2011, pp. 106-109.

[3] L. Manolis Sherman, The New Lightweights: Injection Molded 'Hybrid' Composites Spur Automotive Innovation, *Plastics Technology,* **Vol. 58**, **No. 11**, pp. 22-31.

[4] N. Modler, W. Hufenbach, J. Maaß, A. Liebsch, J. Troschitz and C. Vogel, Werkstoffgerechte Fügesysteme für Strukturbauteile in Mischbauweise, *Proceedings Car Body Colloquium 2014, Chemnitz, 08.-09. Oktober 2014.*

[5] P. A. Cundall and O. D. Starck, A discrete numerical model for granular assemblies, *Geotechnique,* **Vol. 29**, **No. 1**, 1979, pp. 47-65

[6] H. P. Zhu, Z. Y. Zhou, R. Y. Yang and A. B. Yu, Discrete particle simulation of particulate systems: Theoretical developments, *Chemical Engineering Science*, **Vol. 62**, **No. 13**, 2007, pp. 3378-3396

[7] C. Jakob and H. Konietzky, Partikelmethoden – eine Übersicht, *Technische Universität Bergakademie Freiberg*, Freiberg, 2012

[8] Dassault Systèmes, *Abaqus 6.13 Analysis User's Guide*, Providence, Rhode Island, 2013.

[9] C. Höfler, *Entwicklung eines Smoothed Particle Hydrodynamics (SPH) Codes zur numerischen Vorhersage des Primärzerfalls an Brennstoffeinspritzdüsen*, Diss., Karlsruhe, 2013.

[10] J. F. Price, *Lagrangian and Eulerian Representations of Fluid Flow: Kinematics and the Equations of Motion*, Woods Hole, Massachusetts, 2006

[11] Autodesk, *Autodesk simulation moldflow Insight 2014*, San Rafael, California, 2014.

[12] J. Kozicki and J. Tejchmann, Numerical simulations of sand behaviour using DEM with two different descriptions of grain roughness, *Proceedings of the 2nd International Conference on Particle-based Methods – Fundamentals and Applications, PARTICLES 2011 (Eds. E. Oñate and D.R.J. Owen), Barcelona, Spain, October 26-28, 2011,* International Center for Numerical Methods in Engineering (CIMNE), Barcelona, 2011, pp. 62-71.

[13] Y. C. Zhou, B. h. Xu, R. P. Zou, A. B. Yu and P. Zulli, Stress distribution in a sandpile formed on a deflected base, *Advanced Powder Technology,* **Vol. 14, No. 4**, 2003, pp. 401-410.

[14] C. O'Sullivan and J. D. Bray, Selecting a suitable time step for discrete element simulations that use the central difference time integration scheme, *Engineering Computations,* **Vol. 21 No2/3/4**, 2004, pp. 278-303.

[15] M. Chizari, S. T. S. Al-Hassani, L. M. Barrett, Experimental and numerical study of water jet spot welding, *journal of materials processing technology*, **Vol. 198**, 2008, pp. 213-219.